SUPPLEMENTAL INFORMATION

Fructose-1,6-bisphosphatase 2 inhibits sarcoma progression by restraining mitochondrial biogenesis

Peiwei Huangyang, Fuming Li, Pearl Lee, Itzhak Nissim, Aalim M. Weljie, Anthony Mancuso, Bo Li, Brian Keith, Sam S. Yoon, M. Celeste Simon

Supplemental information includes seven figures and one table.

Figure S1

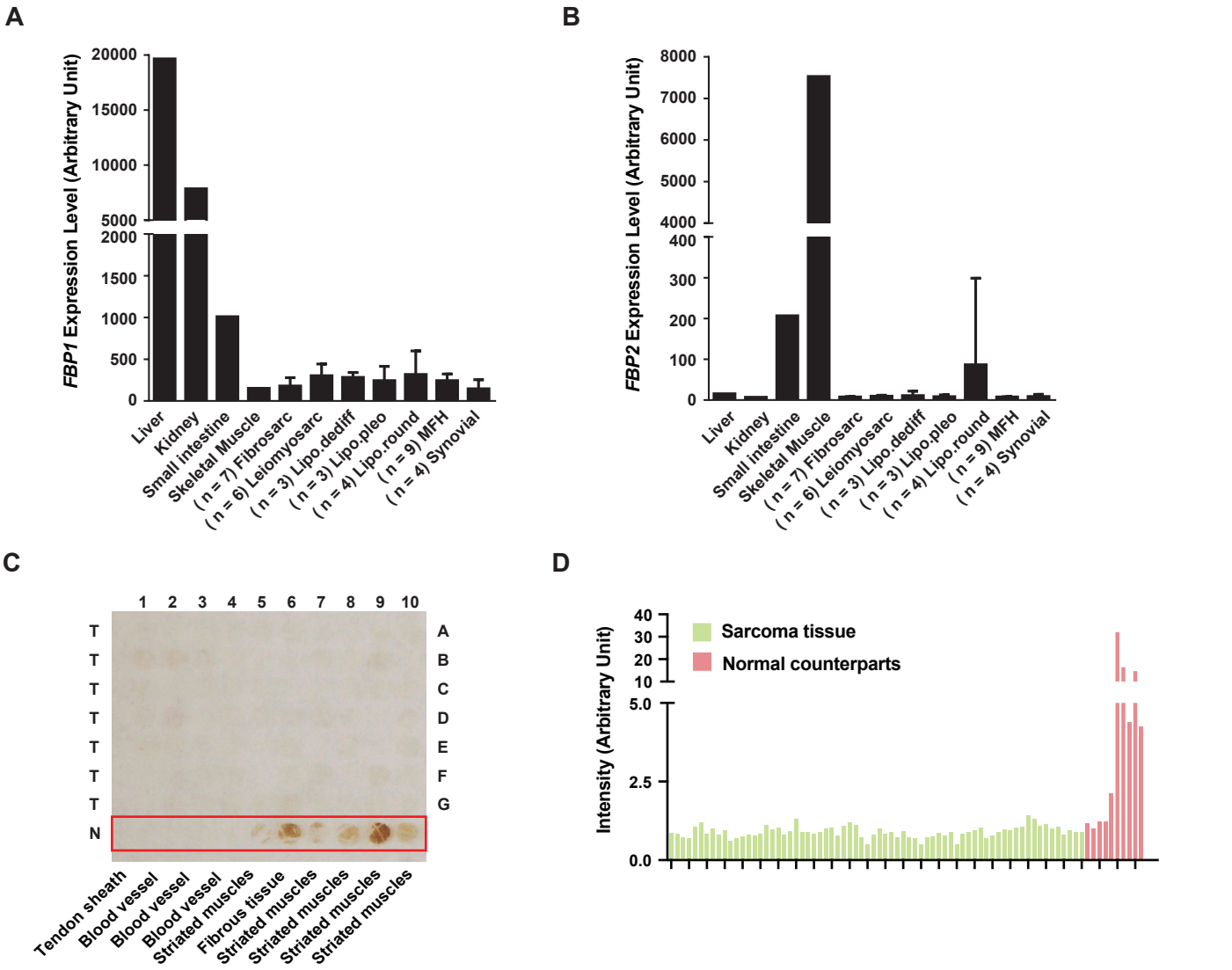

A1: neurofibroma	C1: neurilemmoma	E1: pleomorphic rhabdomyosarcoma	G1: fibrous histiocytoma
A2: leiomyosarcoma	C2: neurilemmoma	E2: hemangioendothelial sarcoma	G2: mucoid type liposarcoma
A3: fibroma	C3: neurilemmoma	E3: liposarcoma	G3: mucoid type liposarcoma
A4: alveolar soft part sarcoma	C4: neurilemmoma	E4: mucoid type liposarcoma	G4: alveolar soft part sarcoma
A5: fibrous histiocytoma	C5: alveolar rhabdomyosarcoma	E5: liposarcoma	G5: fibrous histiocytoma
A6: glomus tumor	C6: neurilemmoma	E6: liposarcoma	G6: fibrous histiocytoma
A7: rhabdomyosarcoma	C7: neurilemmoma	E7: lipoma-like liposarcoma	G7: fibrous histiocytoma
A8: leiomyosarcoma	C8: fibrous histiocytoma	E8: mucoid type liposarcoma	G8: fibrous histiocytoma
A9: leiomyosarcoma	C9: neurilemmoma	E9: lipoma-like liposarcoma	G9: fibrous histiocytoma
A10: leiomyosarcoma	C10: neurilemmoma	E10: fibrous histiocytoma	G10: neurilemmoma
B1: leiomyosarcoma	D1: pleomorphic leiomyosarcoma	F1: fibrous histiocytoma	
B2: leiomyosarcoma	D2: synovial sarcoma	F2: pleomorphic liposarcoma	
B3: neurofibroma	D3: synovioma	F3: pleomorphic liposarcoma	
B4: osteosarcoma	D4: synovial sarcoma	F4: mucoid type liposarcoma	
B5: leiomyosarcoma	D5: synovial sarcoma	F5: lipoma-like liposarcoma	
B6: leiomyosarcoma	D6: tenosynovial giant cell tumor	F6: mucoid type liposarcoma	
B7: neurilemmoma	D7: embryonic rhabdomyosarcoma	F7: round cells liposarcoma	
B8: neurilemmoma	D8: round cells liposarcoma	F8: mucoid type liposarcoma	
B9: neurilemmoma	D9: epithelioid hemangioendothelioma	F9: alveolar rhabdomyosarcoma	
B10: neurofibroma	D10: hemangiopericytoma	F10: alveolar soft tissue sarcoma	

Figure S1, Related to Figure 1. *FBP2* expression is downregulated in sarcoma.

(A and B) *FBP1* (A) and *FBP2* (B) mRNA expression in multiple normal tissues and a variety of human sarcoma samples. Fibrosarc, fibrosarcoma; Lipo.dediff, dedifferentiated liposarcoma; Lipo.pleo, pleomorphic liposarcoma; Lipo.round, round cell liposarcoma; MFH, malignant fibrous histiocytoma.

(C) Immunohistochemistry staining of a representative sarcoma microarray with FBP2 antibody. T, sarcoma tumor tissues; N, normal counterparts. Red box indicates normal counterparts. The sarcoma type of each sample is listed below.

(D) Quantification of IHC staining of 70 sarcomas and 10 normal tissues with FBP2 antibody from (C).

Figure S2

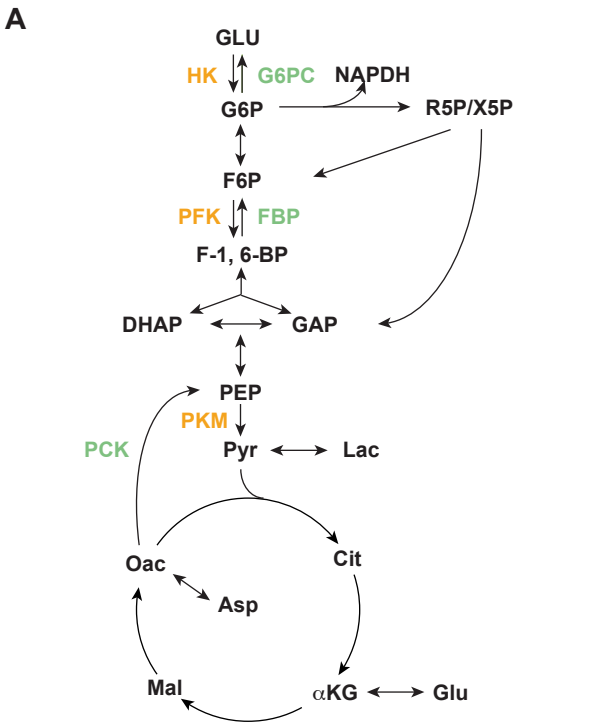
A
GLU
HK
G6PC
NAPDH
G6P
R5P/X5P
F6P
PFK
FBP
F-1, 6-BP
DHAP
GAP
PEP
PKM
PCK
Pyr
Lac
Oac
Cit
Asp
Mal
αKG
Glu

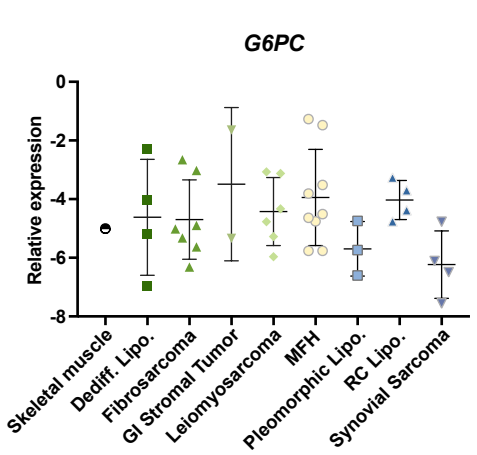
B
G6PC
Relative expression
0
-2
-4
-6
-8
Skeletal muscle
Dediff. Lipo.
Fibrosarcoma
GI Stromal Tumor
Leiomyosarcoma
MFH
Pleomorphic Lipo.
RC Lipo.
Synovial Sarcoma

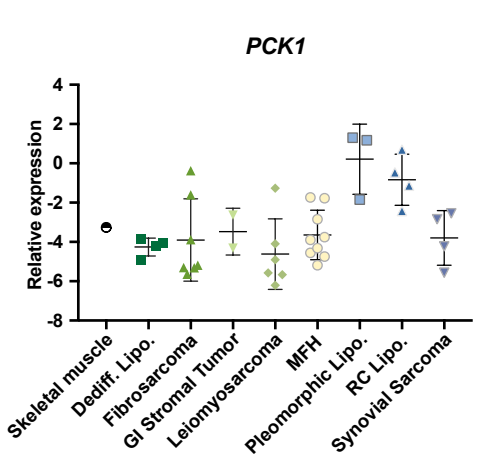
C
PCK1
Relative expression
4
2
0
-2
-4
-6
-8
Skeletal muscle
Dediff. Lipo.
Fibrosarcoma
GI Stromal Tumor
Leiomyosarcoma
MFH
Pleomorphic Lipo.
RC Lipo.
Synovial Sarcoma

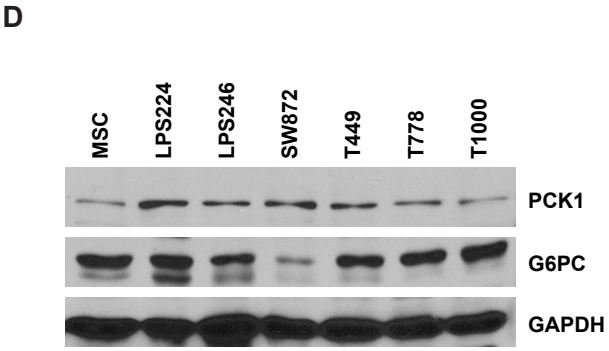
D
MSC
LPS224
LPS246
SW872
T449
T778
T1000
PCK1
G6PC
GAPDH

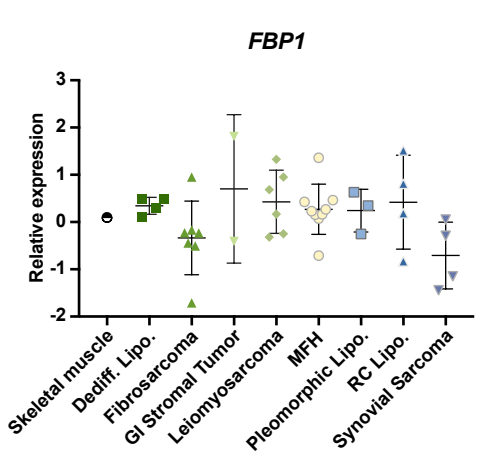
E
FBP1
Relative expression
3
2
1
0
-1
-2
Skeletal muscle
Dediff. Lipo.
Fibrosarcoma
GI Stromal Tumor
Leiomyosarcoma
MFH
Pleomorphic Lipo.
RC Lipo.
Synovial Sarcoma

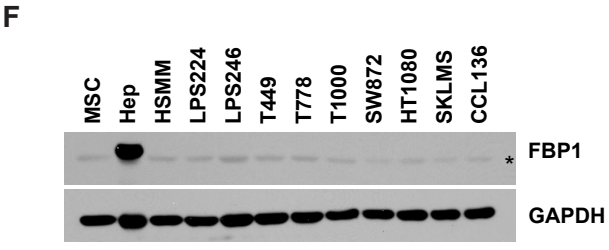
F
MSC
Hep
HSMM
LPS224
LPS246
T449
T778
T1000
SW872
HT1080
SKLMS
CCL136
FBP1
*
GAPDH

Figure S2, Related to Figure 1. The expression of other gluconeogenic enzymes exhibit no consistent change in sarcoma.

(A) Illustration of central carbon metabolism, including glycolysis, gluconeogenesis, pentose phosphate pathway, and the TCA cycle. Enzymes controlling glycolysis (HK, hexokinase; PFK, phosphofructokinase; PKM, pyruvate kinase type M) are highlighted in orange, while enzymes controlling gluconeogenesis (G6PC, glucose-6-phosphatase catalytic subunit; FBP, fructose-1,6-bisphosphatase; PCK, phosphoenolpyruvate carboxykinase) are highlighted in green. G6P, glucose-6-phosphate; F6P, fructose 6-phosphate; F-1,6-BP, fructose 1,6-bisphosphate; DHAP, dihydroxyacetone phosphate; GAP, glyceraldehyde 3-phosphate; R5P, ribose 5-phosphate; X5P, xylulose 5-phosphate; PEP, phosphoenolpyruvate; Pyr, pyruvate; Lac, lactate; Cit, citrate; αKG, α-ketoglutarate; Glu, glutamate; Mal, malate; Oac, oxaloacetate; Asp, aspartate.

(B and C) *G6PC* (B) and *PCK1* (C) mRNA expression based on Oncomine analysis of the Detwiller *et al.* sarcoma patient samples data set (Detwiller et al., 2005). Values are normalized to median-centered intensity and shown on a $\log_2$ scale. Dediff. lipo., dedifferentiated liposarcoma; MFH, Malignant Fibrous Histiocytoma; Pleomorphic lipo., pleomorphic liposarcoma; RC lipo., round cell liposarcoma.

(D) Immunoblot analysis of PCK1 and G6PC protein levels in various human sarcoma cell lines. MSC, mesenchymal stem cells. MSCs served as normal control, while GAPDH served as a loading control.

(E) *FBP1* mRNA expression based on Oncomine analysis of the Detwiller *et al.* sarcoma patient samples data set (Detwiller et al., 2005).

(F) Immunoblot analysis of FBP1 protein levels in various human sarcoma cell lines. MSC, mesenchymal stem cell; hep, human primary hepatocyte. MSC served as normal control and Hep served as positive control for FBP1 expression. GAPDH served as a loading control. * indicates non-specific band.

Figure S3

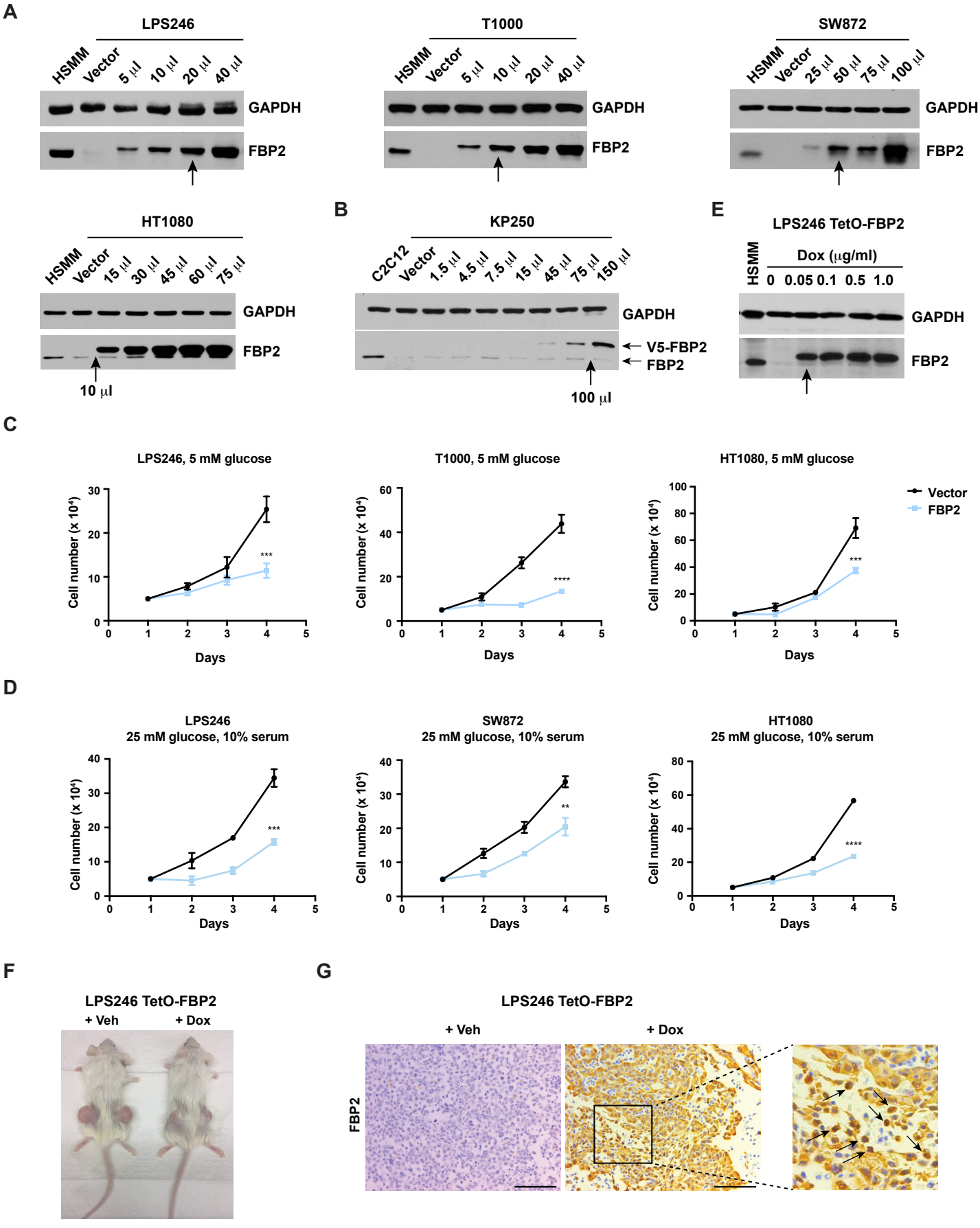
A
LPS246
HSMM
Vector
5 μl
10 μl
20 μl
40 μl
GAPDH
FBP2
T1000
HSMM
Vector
5 μl
10 μl
20 μl
40 μl
GAPDH
FBP2
SW872
HSMM
Vector
25 μl
50 μl
75 μl
100 μl
GAPDH
FBP2
HT1080
HSMM
Vector
15 μl
30 μl
45 μl
60 μl
75 μl
GAPDH
FBP2
10 μl
B
KP250
C2C12
Vector
1.5 μl
4.5 μl
7.5 μl
15 μl
45 μl
75 μl
150 μl
GAPDH
V5-FBP2
FBP2
100 μl
E
LPS246 TetO-FBP2
HSMM
Dox (μg/ml)
0 0.05 0.1 0.5 1.0
GAPDH
FBP2
C
LPS246, 5 mM glucose
T1000, 5 mM glucose
HT1080, 5 mM glucose
Cell number (x 10⁴)
Days
Vector
FBP2
***
****
D
LPS246
25 mM glucose, 10% serum
SW872
25 mM glucose, 10% serum
HT1080
25 mM glucose, 10% serum
Cell number (x 10⁴)
Days
F
LPS246 TetO-FBP2
+ Veh
+ Dox
G
LPS246 TetO-FBP2
+ Veh
+ Dox
FBP2

Figure S3, Related to Figure 2. FBP2 re-expression inhibits tumor growth.

(A and B) Immunoblot showing FBP2 expression levels over lentiviral titration in LPS246, T1000, SW872 and HT1080 cells compared to HSMM (A), and in KP250 cells compared to C2C12 (B). GAPDH served as a loading control. Arrows indicate virus volumes used for all experiments.

(C and D) Growth of LPS246, T1000, and HT1080 cells in low glucose medium (10% FBS and 5 mM glucose) (C) and replete medium (10% FBS and 25 mM glucose) (D), with or without ectopic FBP2 expression. n = 3, *p < 0.05, **p < 0.01, ***p < 0.001, ****p < 0.0001.

(E) Immunoblot showing FBP2 expression level with increased doxycycline concentration in LPS246 cells compared to HSMM. GAPDH served as loading control. The arrow indicates dox concentration used for all experiments.

(F) Representative xenograft tumors in mice fed with vehicle or dox chow.

(G) Representative immunohistochemistry image of FBP2 staining on LPS246 TetO-FBP2 tumor sections. Scale bars: 100 μm. Arrows indicate nuclear staining of FBP2.

Error bars represent SD of three experimental replicates. *p < 0.05, **p < 0.01, ***p < 0.001, ****p < 0.0001. n.s., not significant.

Figure S4

A

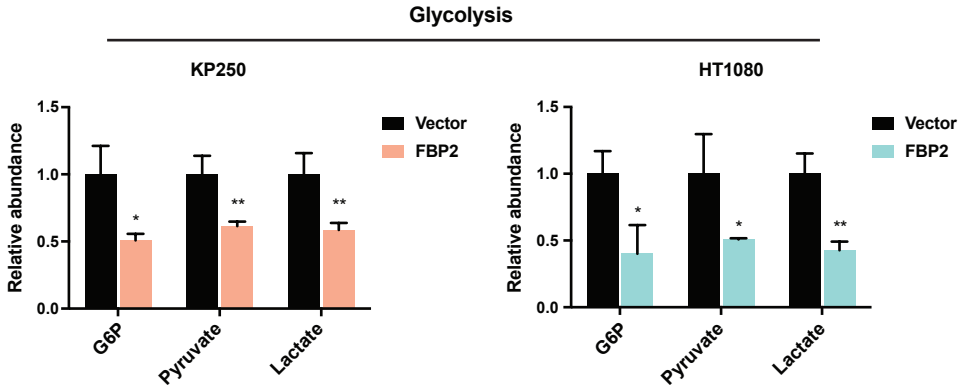

B

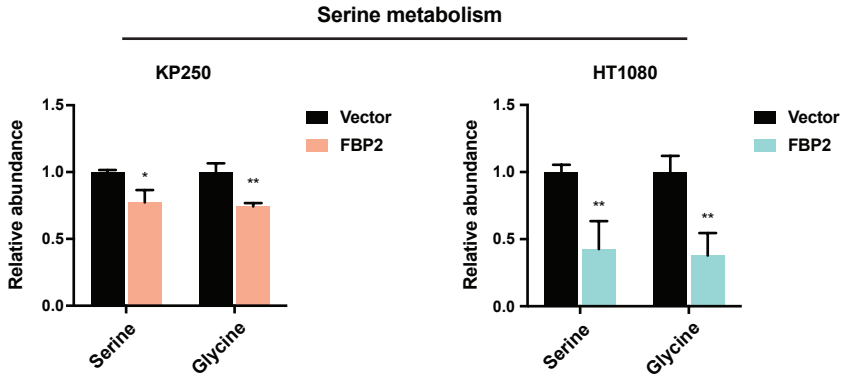

C

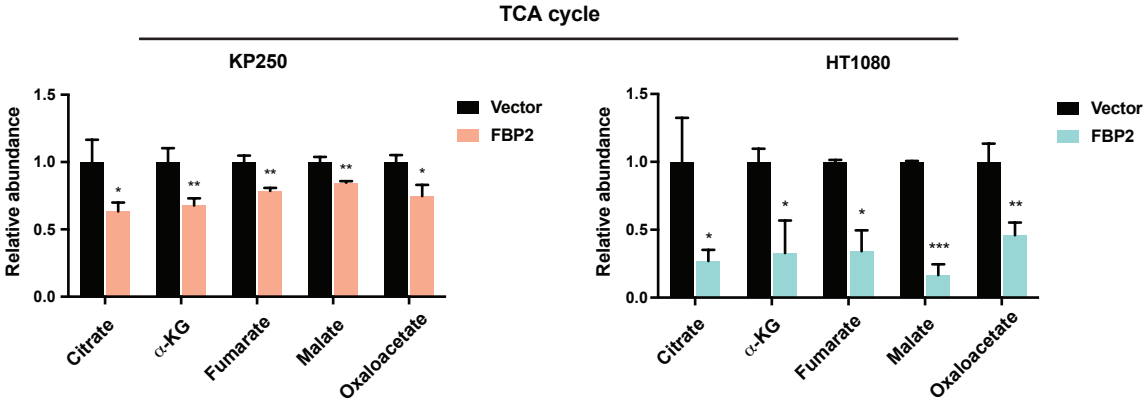

D

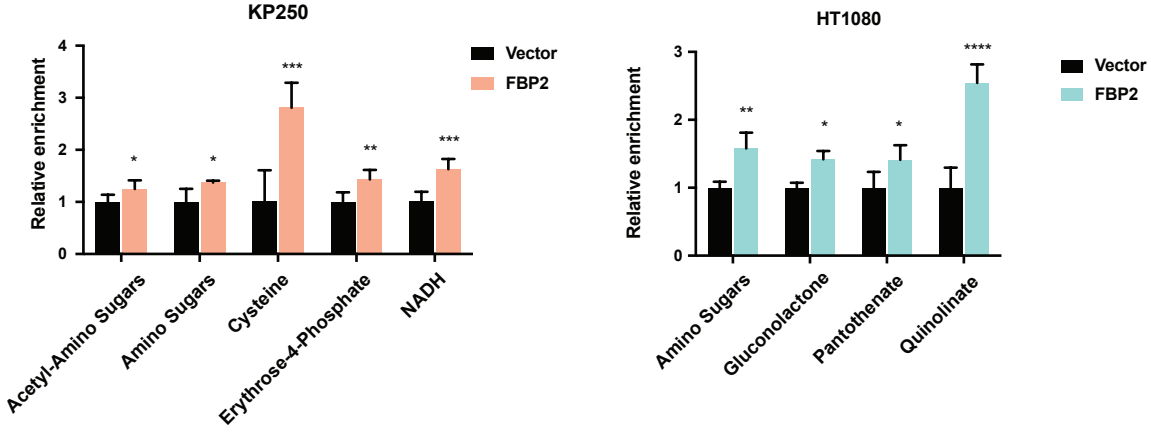

Figure S4, Related to Figure 3. Ectopic FBP2 expression opposes glycolysis and the TCA cycle.

(A-C) Pan-metabolomic analysis of steady-state metabolites in KP250 cells (left) and HT1080 cells (right) expressing vector control or FBP2. Relative abundance of metabolites in glycolysis (A), serine metabolism (B) and TCA cycle (C) are shown.

(D) Representative examples of metabolites whose relative abundance is higher in KP250 cells (left) or HT1080 cells (right) upon FBP2 restoration, compared to cells expressing control vector.

Error bars represent SD of three experimental replicates. *$p < 0.05$, **$p < 0.01$, ***$p < 0.001$, ****$p < 0.0001$. n.s., not significant.

Figure S5

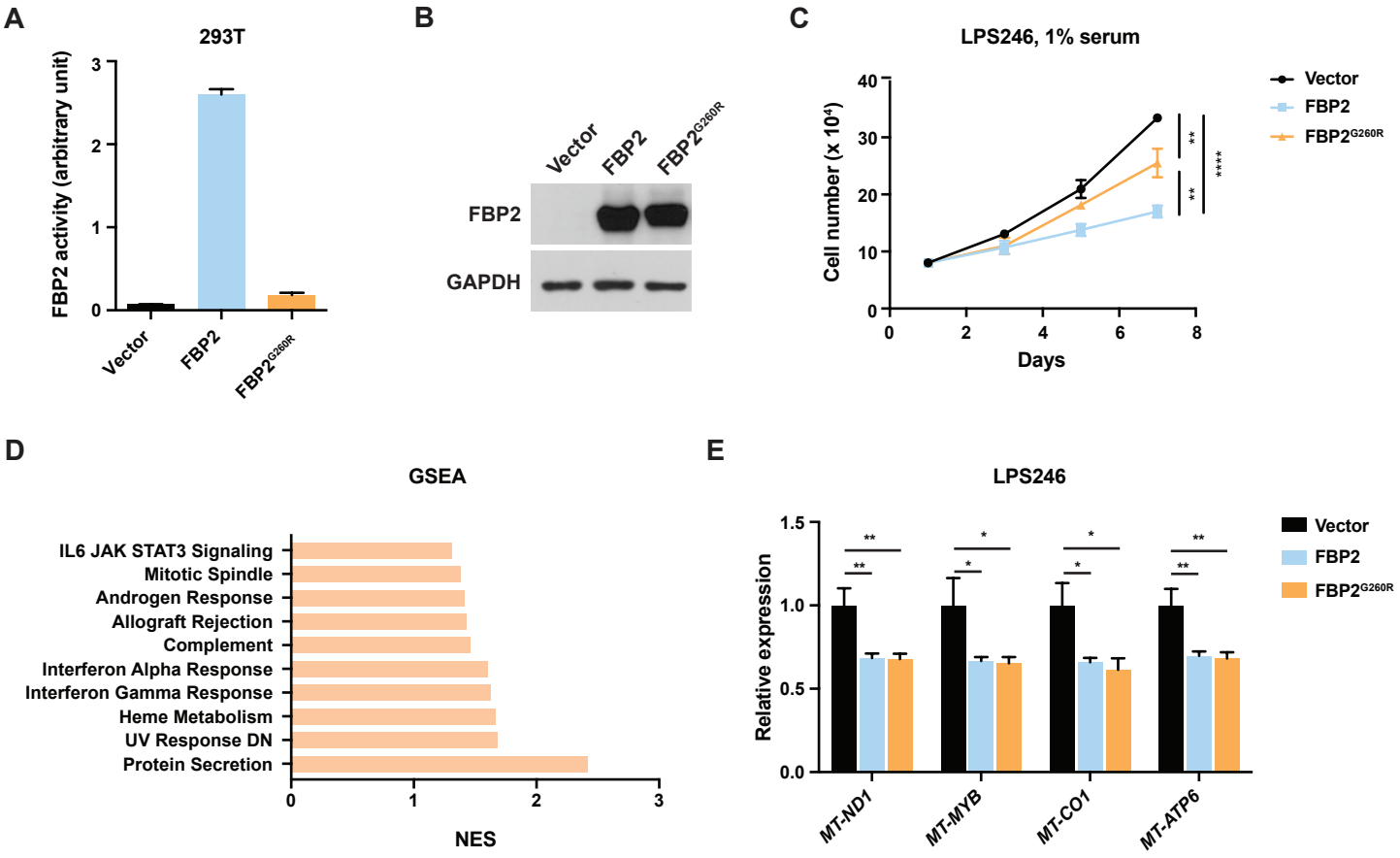

Figure S5, Related to Figure 4. FBP2 inhibits mitochondrial gene expression in a catalytic activity-independent manner.

(A) Enzymatic activity of FBP2 in 293T cells expressing vector, wild-type FBP2 and FBP2^{G260R}.

(B) Protein levels of ectopically expressed FBP2 and FBP2^{G260R} in LPS246 cells. GAPDH was used as a loading control.

(C) Growth of vector control, FBP2- or FBP2^{G260R}-expressing LPS246 cells grown in 1% serum medium.

(D) GSEA comparing vehicle-treated (n = 5) and dox-treated (n = 4) LPS246 TetO-FBP2 cells. The 50-gene "Hallmark signatures" set from MsigDB was queried, revealing top 10 gene sets upregulated in dox-treated groups, as shown with the normalized enrichment score (NES).

(E) qRT-PCR analysis of *MT-ND1*, *MT-CYB*, *MT-CO1*, and *MT-ATP6* in LPS246 cells constitutively expressing vector, FBP2 or FBP2^{G260R}.

Error bars represent SD of three experimental replicates. *p < 0.05, **p < 0.01, ***p < 0.001, ****p < 0.0001. n.s., not significant.

Figure S6

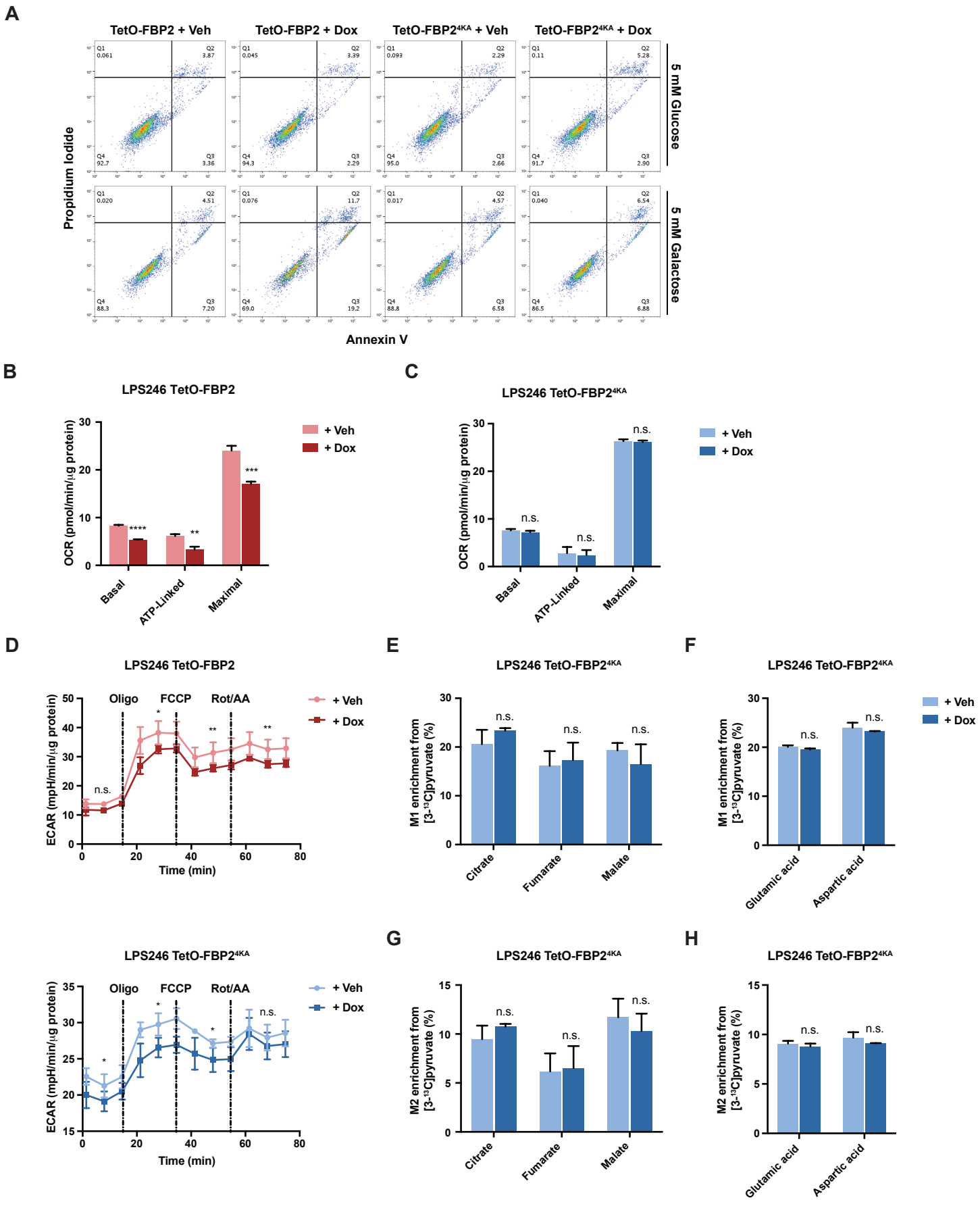
A
TetO-FBP2 + Veh
TetO-FBP2 + Dox
TetO-FBP2^4KA + Veh
TetO-FBP2^4KA + Dox
5 mM Glucose
5 mM Galactose
Propidium Iodide
Annexin V
B
LPS246 TetO-FBP2
OCR (pmol/min/μg protein)
+ Veh
+ Dox
Basal
ATP-Linked
Maximal
C
LPS246 TetO-FBP2^4KA
n.s.
D
LPS246 TetO-FBP2
ECAR (mpH/min/μg protein)
Oligo
FCCP
Rot/AA
Time (min)
E
LPS246 TetO-FBP2^4KA
M1 enrichment from [3-13C]pyruvate (%)
Citrate
Fumarate
Malate
F
LPS246 TetO-FBP2^4KA
Glutamic acid
Aspartic acid
G
LPS246 TetO-FBP2^4KA
M2 enrichment from [3-13C]pyruvate (%)
H
LPS246 TetO-FBP2^4KA

Figure S6, Related to Figure 6. FBP2 re-expression affects mitochondrial respiratory capacity.

(A) Indicated cells were cultured in 5 mM glucose and 5 mM galactose medium. Flow cytometry plots of Annexin V/PI staining of indicated cells.

(B and C) Histogram showing basal, ATP-linked and maximal respiration in LPS246 TetO-FBP2 cells (B) or LPS246 TetO-FBP2^{4KA} cells (C) treated with vehicle or dox. Data are presented as mean ± SD of three reading cycles of n = 9 wells pooled from three independent experiments. **p < 0.01, ***p < 0.001, ****p < 0.0001.

(D) Relative extracellular acidification rate (ECAR) normalized to protein abundance in LPS246 TetO-FBP2 cells (upper panel) or LPS246 TetO-FBP2^{4KA} cells (lower panel) treated with vehicle or dox. Data are presented as mean ± SD of three reading cycles of n = 9 wells pooled from three independent experiments.

(E-H) M1 isotopomer distribution of indicated TCA metabolites (E) and amino acids (F), and M2 isotopomer distribution of indicated TCA metabolites (G) and amino acids (H) in LPS246 TetO-FBP2^{4KA} cells with vehicle or dox treatment, labelled with [3-^{13}C]pyruvate. Error bars represent SD of three experimental replicates. *p < 0.05, **p < 0.01, ***p < 0.001, ****p < 0.0001. n.s., not significant.

Figure S7

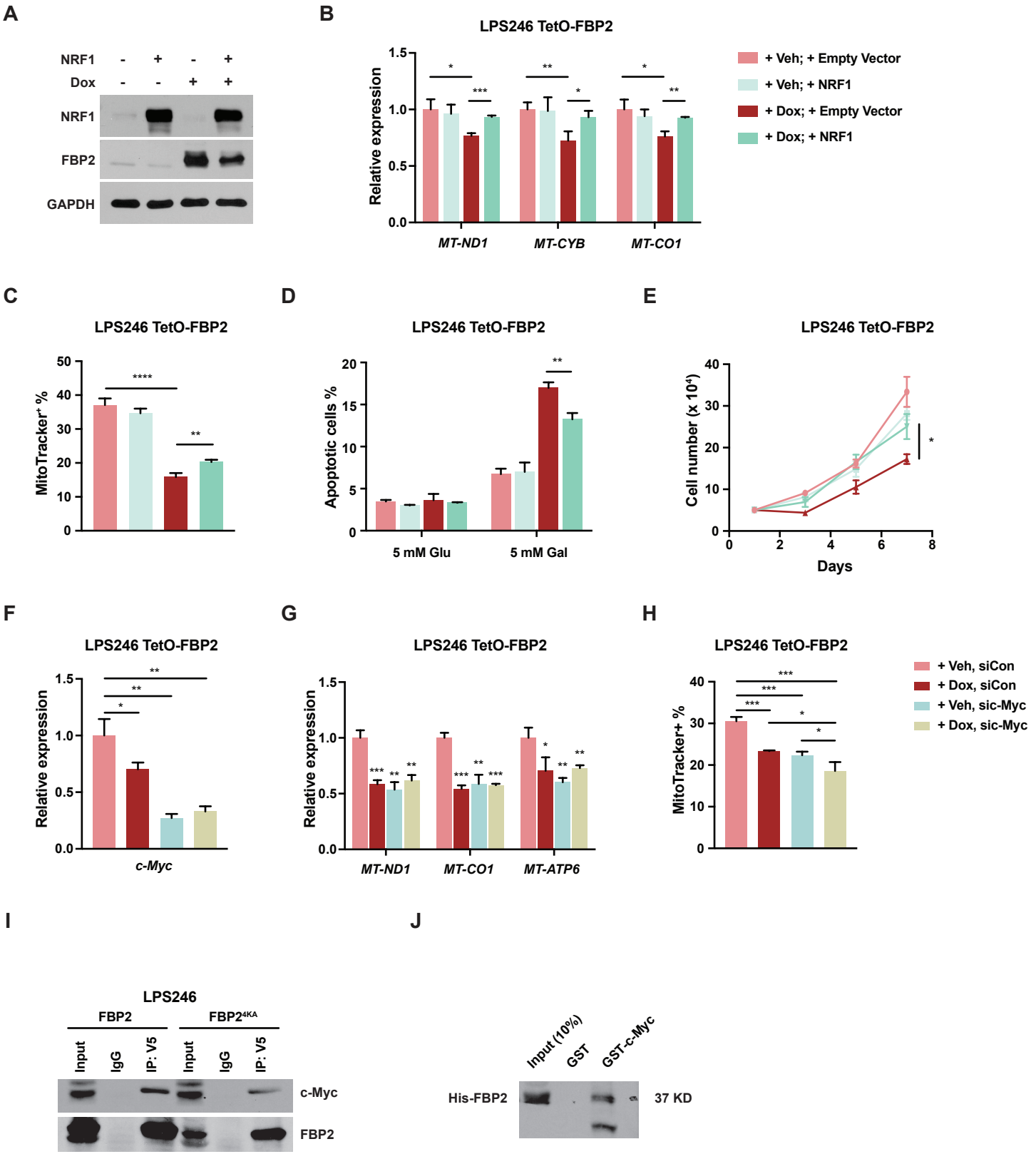
A
NRF1 - + - +
Dox - - + +
NRF1
FBP2
GAPDH
B
LPS246 TetO-FBP2
Relative expression
MT-ND1
MT-CYB
MT-CO1
+ Veh; + Empty Vector
+ Veh; + NRF1
+ Dox; + Empty Vector
+ Dox; + NRF1
C
LPS246 TetO-FBP2
MitoTracker+ %
D
LPS246 TetO-FBP2
Apoptotic cells %
5 mM Glu
5 mM Gal
E
LPS246 TetO-FBP2
Cell number (x 10⁴)
Days
F
LPS246 TetO-FBP2
Relative expression
c-Myc
G
LPS246 TetO-FBP2
Relative expression
MT-ND1
MT-CO1
MT-ATP6
H
LPS246 TetO-FBP2
MitoTracker+ %
+ Veh, siCon
+ Dox, siCon
+ Veh, sic-Myc
+ Dox, sic-Myc
I
LPS246
FBP2
FBP2⁴ᴷᴬ
Input
IgG
IP: V5
c-Myc
FBP2
J
Input (10%)
GST
GST-c-Myc
His-FBP2
37 KD

Figure S7, Related to Figure 7. NRF1 partially rescues FBP2-mediated inhibition of mitochondrial biogenesis; FBP2's effects on mitochondrial biogenesis are highly dependent on c-Myc.

(A) Immunoblot analysis for ectopic expression of vector control or NRF1 in LPS246 TetO-FBP2 cells.

(B) qRT-PCR analysis of *MT-ND1*, *MT-CYB*, and *MT-CO1* in indicated cells.

(C) LPS246 TetO-FBP2 cells with or without NRF1 expression were stained with MitoTracker Green FM probe. Fluorescence intensity corresponding to mitochondrial mass is shown in histogram.

(D) Indicated cells were cultured in 5 mM glucose and 5 mM galactose medium. Apoptotic cells were measured through Annexin V/PI staining followed by flow cytometry.

(E) Growth of indicated cells in low serum medium (1% FBS).

(F and G) qRT-PCR analysis of *c-Myc* (F) and *MT-ND1*, *MT-CO1* and *MT-ATP6* (G) in LPS246 TetO-FBP2 cells under four conditions (+ Veh, siControl; + Dox, siControl; + Veh, sic-Myc; + Dox, sic-Myc).

(H) LPS246 TetO-FBP2 cells treated with four conditions stained with MitoTracker Green FM probe. Histogram shows the quantification of fluorescence intensity corresponding to mitochondrial mass.

(I) V5 tagged FBP2 or FBP2^{4KA}-expressing LPS246 cell lysates were immunoprecipitated with IgG, or V5 antibody and blotted for endogenous c-Myc. IP, immunoprecipitate.

(J) GST pull-down analysis between recombinant His-FBP2 and recombinant GST or GST-tagged c-Myc and blotted using FBP2 antibody.

Error bars represent SD of three experimental replicates. *$p < 0.05$, **$p < 0.01$, ***$p < 0.001$, ****$p < 0.0001$. n.s., not significant.

Table S1. Related to STAR METHODS section. Primers for qRT-PCR.

18S	Life Technologies	HS03928985_G1
MT-ND1	Life Technologies	HS02596873_S1
MT-MYB	Life Technologies	HS02596867_S1
MT-CO1	Life Technologies	HS02596864_G1
MT-ATP6	Life Technologies	HS02596862_G1
TFAM	Life Technologies	Hs00273372_s1
NRF1	Life Technologies	Hs00602161_m1
c-Myc	Life Technologies	Hs00153408_m1
CCDN2	Life Technologies	Hs00153380_m1
eIF2A	Life Technologies	Hs00230684_m1
NPM1	Life Technologies	Hs02339479_g1
PSAT1	Life Technologies	Hs00795278_mH
TFAM_Neg	(Li et al., 2005)	Forward: GATGAATGAGGCAGAATCAGC
		Reverse: CTTTCACCCATCTTGAAGTCC
TFAM_1	(Li et al., 2005)	Forward: GGCATACTTGTCACACGTTCTCA
		Reverse: CAGTCTGGCCTCCAGCTTG
TFAM_2	(Li et al., 2005)	Forward: TTAGGTTTGCGAATCCCCG
		Reverse: CGCCCGTGACGGTCA
β-globin (genomic DNA)	(Dickinson et al., 2013)	Forward: CAACTTCATCCACGTTCACC
		Reverse: GAAGAGCCAAGGACAGGTAC